

POSTER SESSION

P.1 WIND AND WAVES IN THE MIDDLE ATMOSPHERE  
OBSERVED WITH THE MU RADAR

S. Fukao, T. Tsuda, T. Sato, M. Yamamoto, and S. Kato

Radio Atmospheric Science Center  
Kyoto University, UJI Kyoto 611 Japan

The VHF-band MU radar at Shigaraki, Japan, has been in full operation successfully since April 1985. This paper will focus on dynamical features found primarily in the data obtained by the radar during a one-year period from December 1985 to November 1986. These include: basic wind observations, quasi-monochromatic gravity waves generated by the jet stream or through a geostrophic adjustment process, seasonal variation of the mesoscale wind variability, the momentum flux due to gravity wave motions, and saturated gravity wave spectrum. A short discussion will be added to the relationship between turbulent layers and ambient wind field in the mesosphere.

## ZONAL WIND FOUR CONTINUOUS DAY AVERAGE

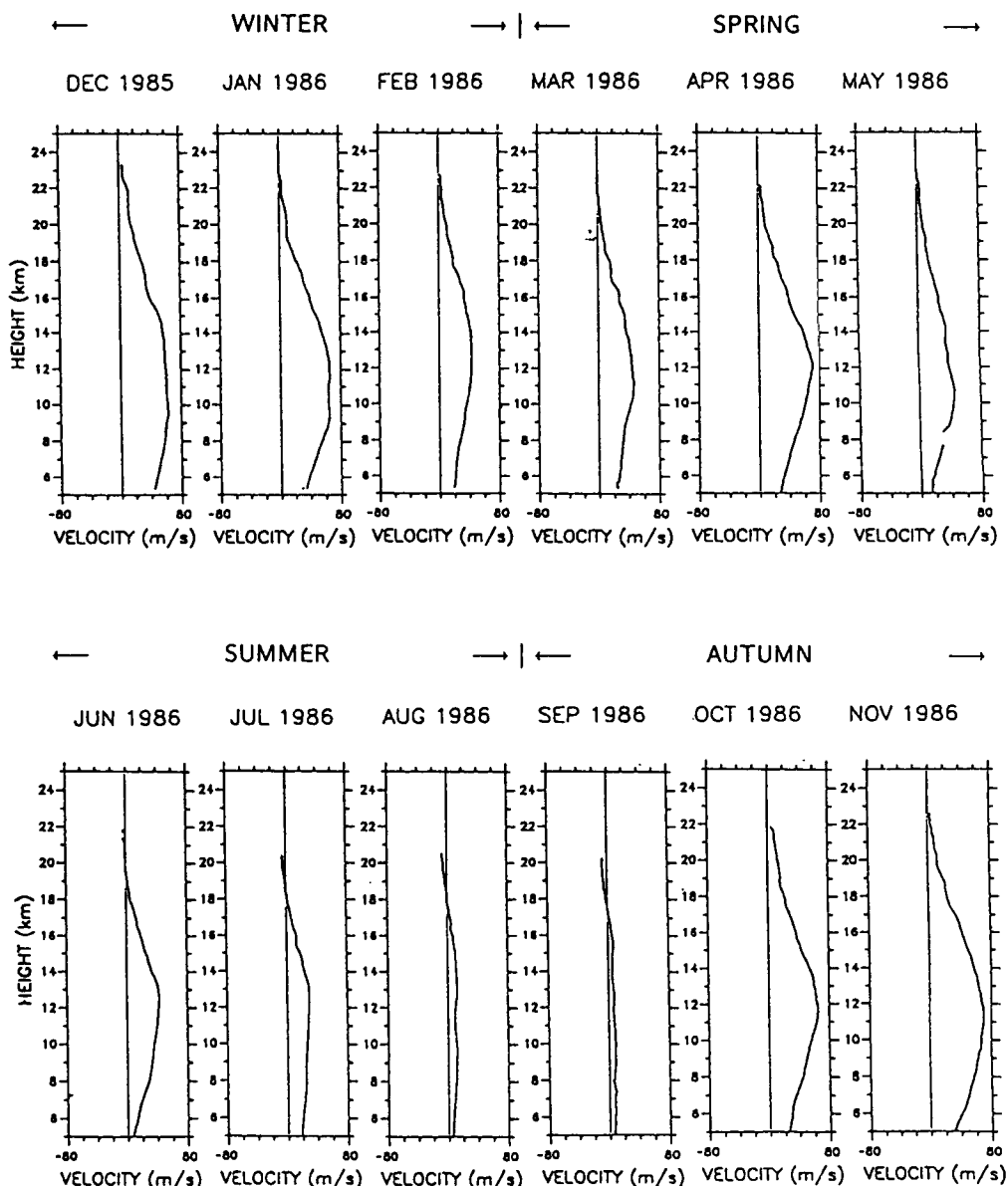


**Figure 1.** Zonal wind averaged over four continuous days each month. A typical seasonal wind change in Japan is observed with the subtropical jet predominating in winter and weak in summer.

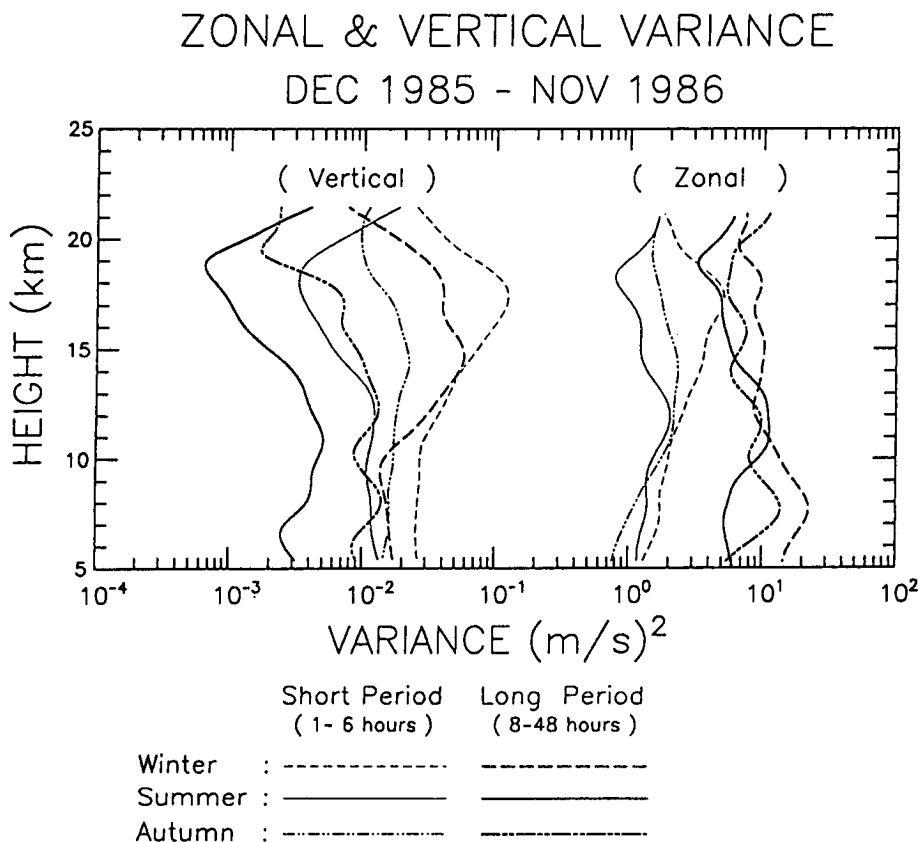


Figure 2. Horizontal and vertical velocity variance for two period ranges during summer, autumn and winter. The gravity wave characteristics are reflected here with wave front being more vertical with increasing periods.

MEAN PSD OF HOURLY MEAN FLUCTUATIONS  
 DEC 1985 - NOV 1986  
 STRATOSPHERE

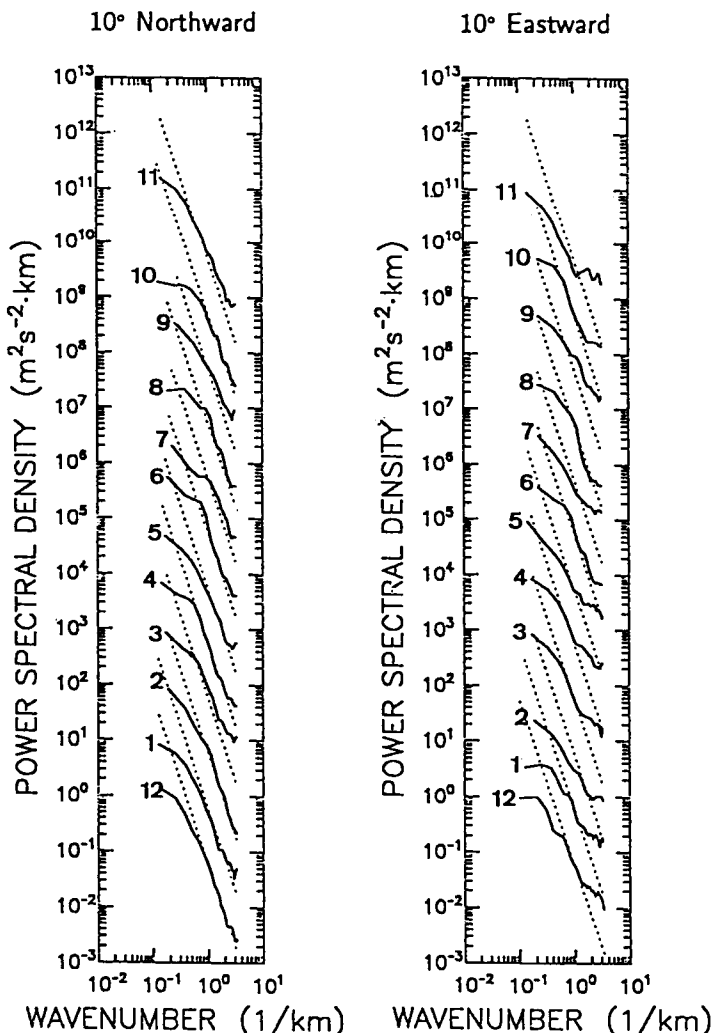


Figure 3. Monthly change of power spectral densities (PSD) of northward and eastward radial velocity in the stratosphere (left) and troposphere (right) compared to a theoretical saturated spectrum. PSD changes little despite the conspicuous seasonal change of the mean wind, suggesting that nonorographic sources are important for middle atmospheric gravity waves.

MEAN PSD OF HOURLY MEAN FLUCTUATIONS  
 DEC 1985 – NOV 1986  
 TROPOSPHERE

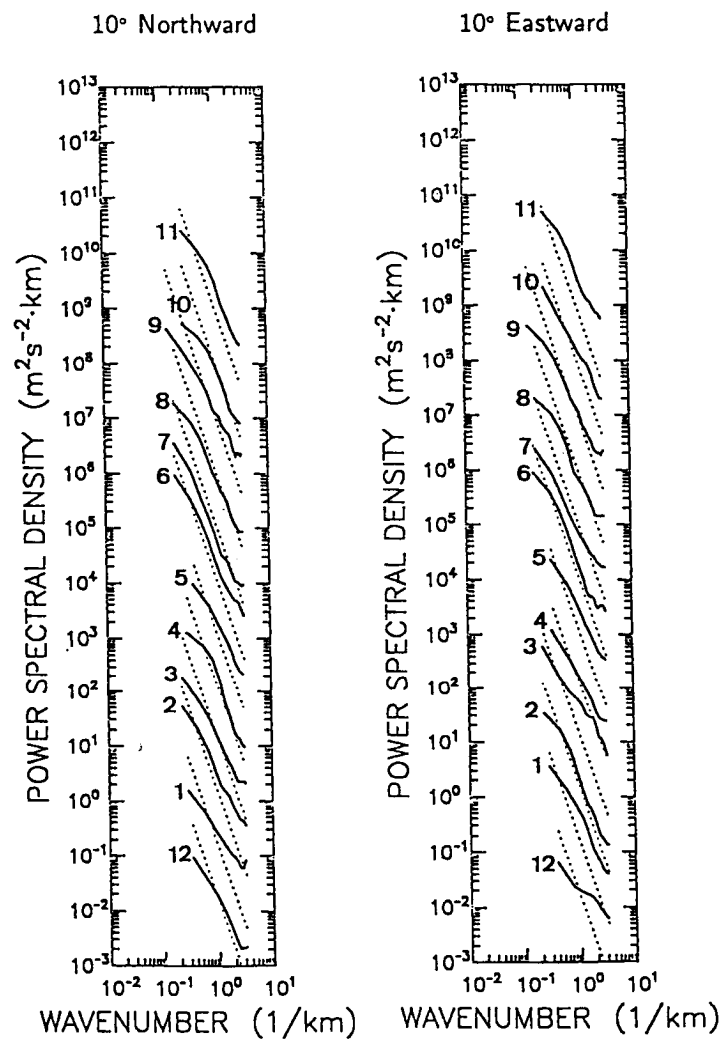


Figure 3. Continued.

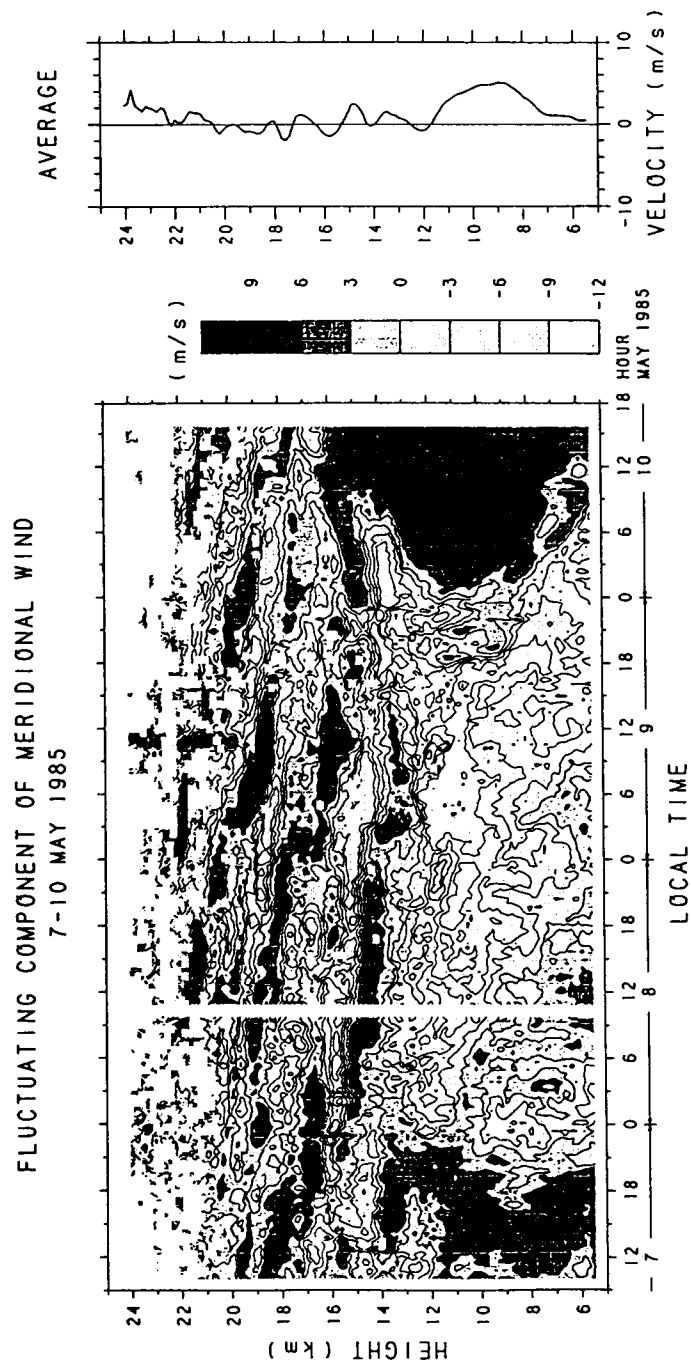


Figure 4. Cross section of meridional wind perturbation relative to the mean wind averaged over the whole observational period.

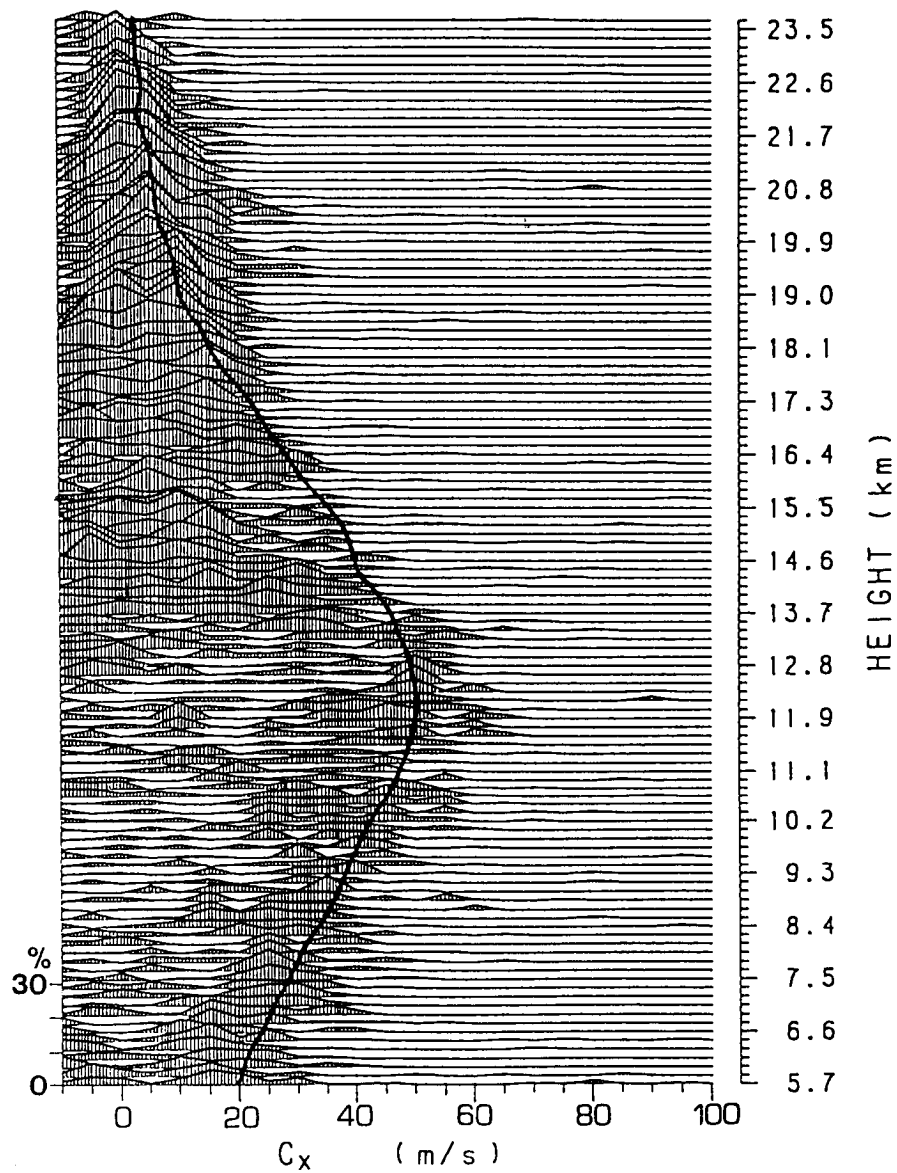


Figure 5. Histogram of the zonal phase velocity analyzed from 30 min average hodographs compared to the mean zonal wind (thick curve). The scale is correct for the lowest spectral curve.

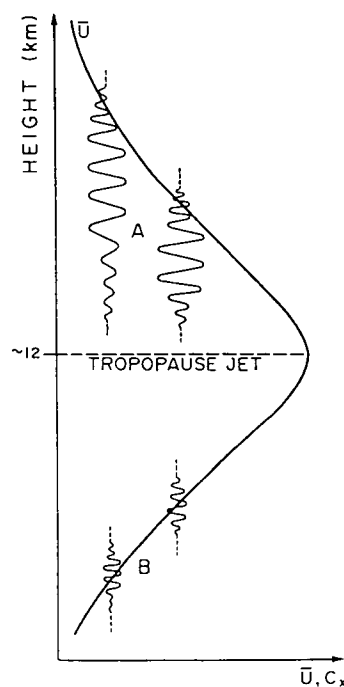


Figure 6. A wave selection model.

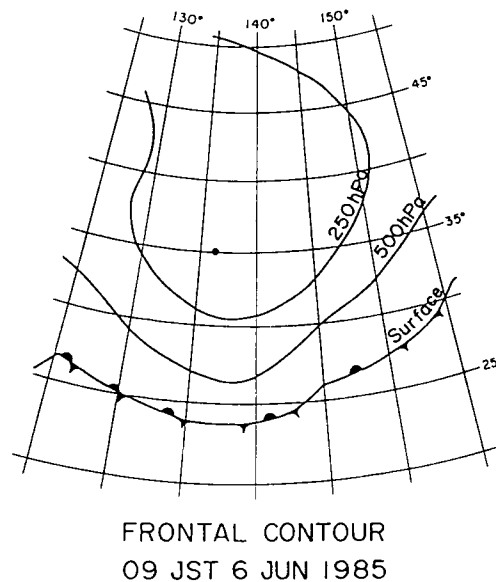


Figure 7. Frontal contours at 09 LST June 1985.

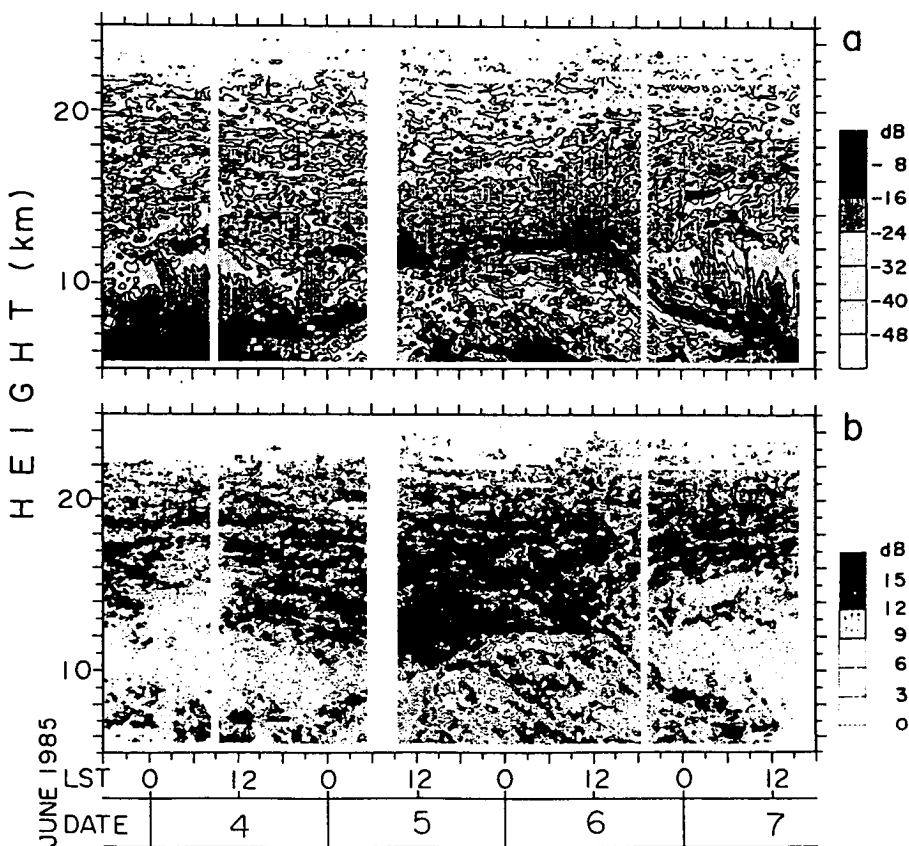


Figure 8. (a) Vertical echo power (in an arbitrary unit) and (b) echo power ratio of the zenith to the  $10^\circ$  oblique direction, showing a structure of the cold air dome.

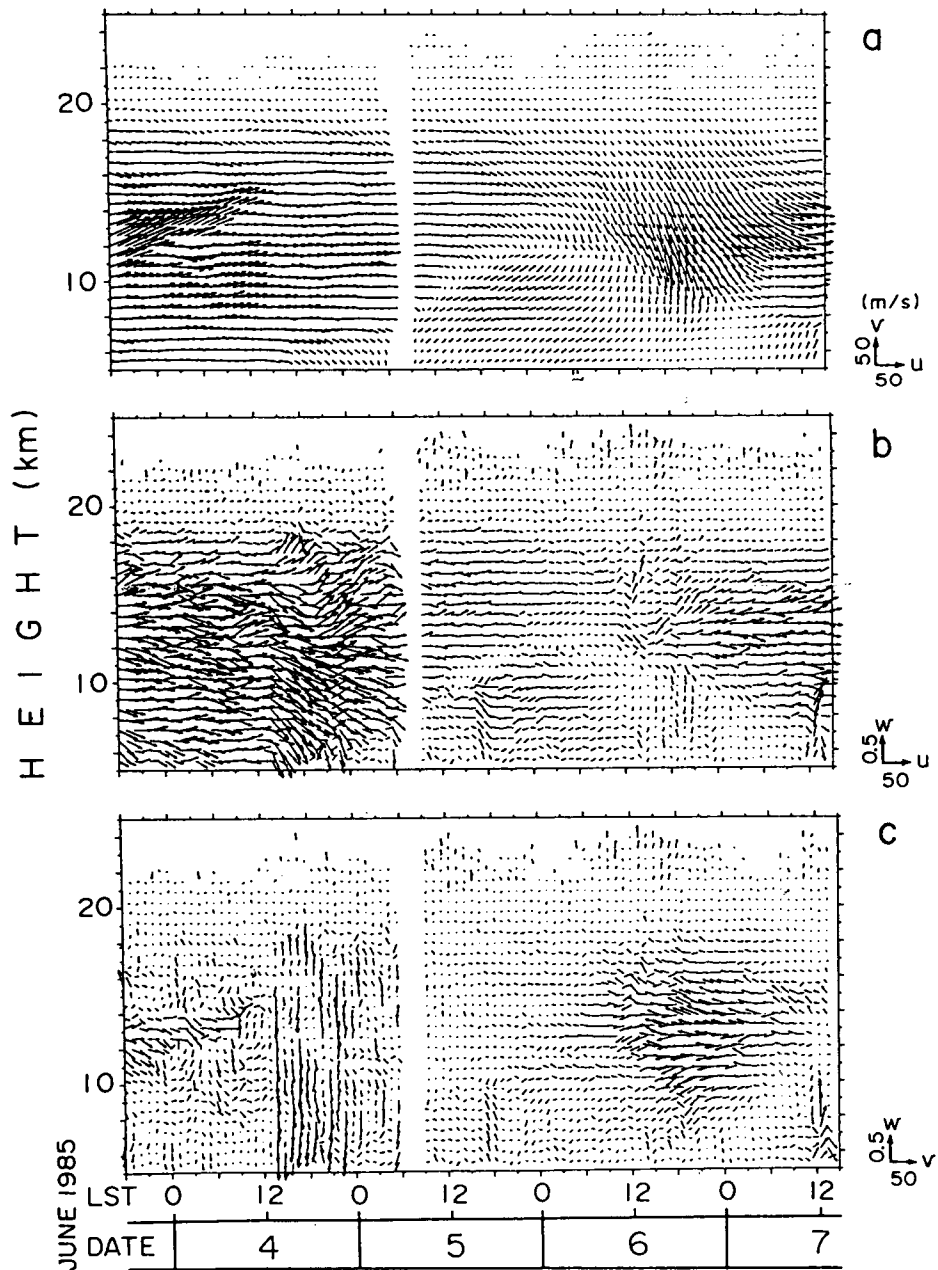


Figure 9. (a) Zonal-meridional, (b) zonal-vertical, and (c) meridional-vertical winds.  $u$ ,  $v$  and  $w$  denote eastward, northward, and upward winds, respectively.

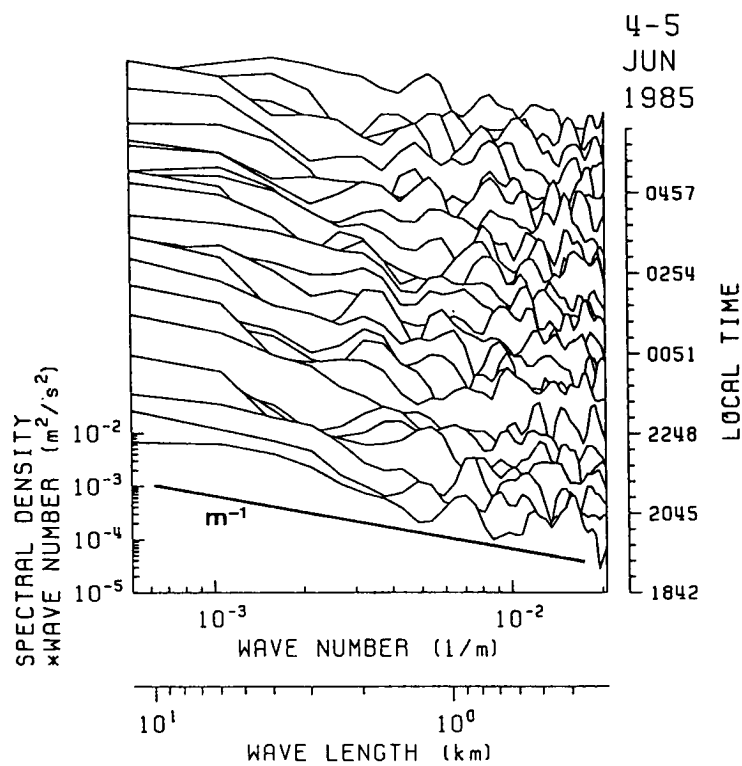


Figure 10. Area-preserving vertical wave number spectra of  $w$ .

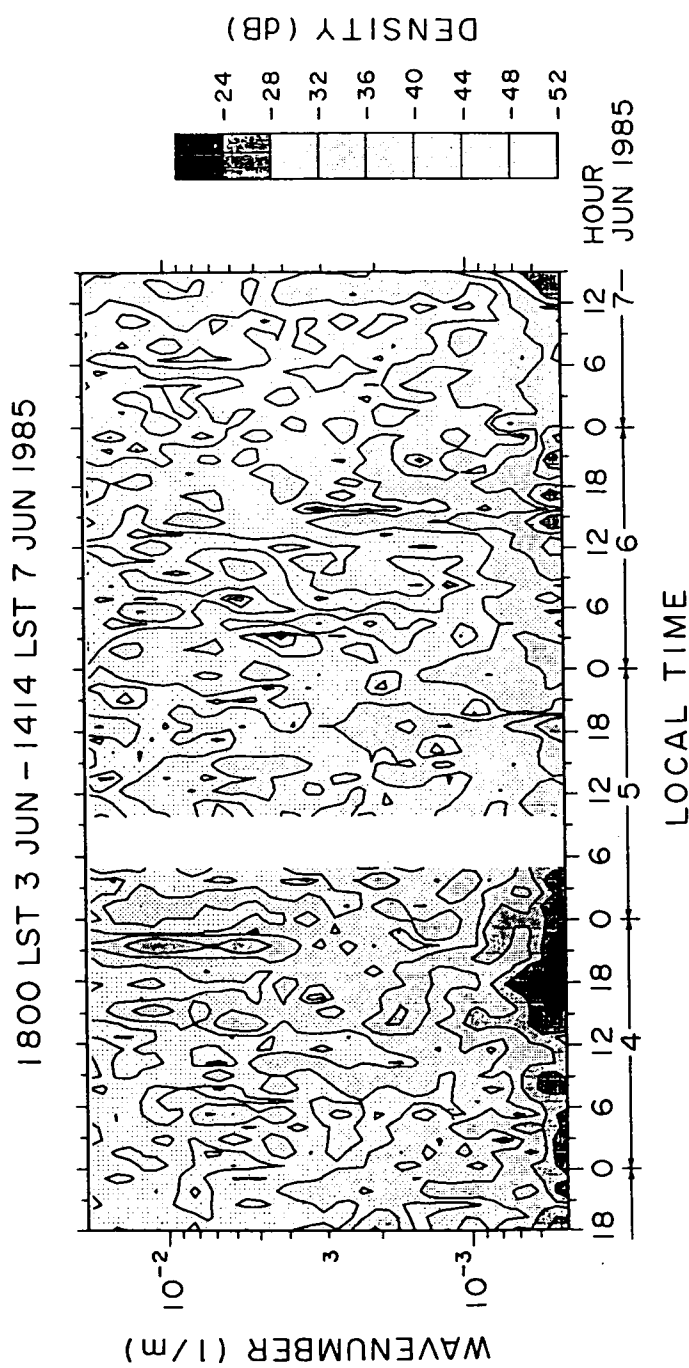


Figure 11. Temporal variation of the area-preserving vertical wave number spectra of  $w$ .